Cognitive Neurodynamics (2019) 13:325–339
https://doi.org/10.1007/s11571-019-09527-y

RESEARCH ARTICLE

Complex network based models of ECoG signals for detection of induced epileptic seizures in rats

Zeynab Mohammadpoory[1] · Mahda Nasrolahzadeh[1] · Naghmeh Mahmoodian[1,3] · Mohammad Sayyah[2] · Javad Haddadnia[1]

Received: 24 November 2017 / Revised: 15 February 2019 / Accepted: 6 March 2019 / Published online: 15 March 2019

Abstract

The automatic detection of seizures bears a considerable significance in epileptic diagnosis as it can efficiently lead to a considerable reduction of the workload of the medical staff. The present study aims at automatic detecting epileptic seizures in epileptic rats. To this end, seizures were induced in rats implementing the pentylenetetrazole model, with the electrocorticogram (ECoG) signals during, before and after the seizure periods being recorded. For this purpose, five algorithms for transforming time series into complex networks based on visibility graph (VG) algorithm were used. In this study, VG based methods were used for the first time to analyze ECoG signals in rats. Afterward, Standard measures in network science (graph properties) were made to examine the topological structure of these networks produced on the basis of ECoG signals. Then these measures were given to a classifier as input features so that the ECoG signals could be classified into seizure periods and seizure-free periods. Artificial Neural Network, considered a popular classifier, was used in this work. The experimental results showed that the method managed to detect epileptic seizure in rats with a high accuracy of 92.13%. Our proposed method was also applied to the recorded EEG signals from Bonn database to show the efficiency of the proposed method for human seizure detection.

Keywords Induced epilepsy · Epileptic rat · Seizure detection · Complex network · Pntylenetetrazole (PTZ)

Introduction

Inflicting around one percent of the total population in the world, Epilepsy, a neurological disorder associated with irregular brain tissue activity which causes seizures, is considered one of the commonest chronic diseases (Firpi et al. 2007). Electroencephalogram (EEG) reflects the electrical activity of the brain, providing a mass of physiological and pathological information (Kristiansen and Courtois 1949). The EEG plays an important role in a variety of epilepsy-related procedures including epilepsy diagnosis, and epileptogenic zone determination helpful for pre-surgical evaluations. The conventional seizure detection procedures, such as the visual inspection of the EEG by a trained neurologist, are quite challenging in that the massive amounts of EEG data involved, and the existence of myogenic artifacts in the signals make the process of

✉ Zeynab Mohammadpoory
z.mohammadpoory@gmail.com

Mahda Nasrolahzadeh
ms.nasrolahzadeh@yahoo.com

Naghmeh Mahmoodian
naghmeh.ma56@yahoo.com

Mohammad Sayyah
Sayyahm2@yahoo.com

Javad Haddadnia
Haddadnia@hsu.ac.ir

[1] Department of Biomedical Engineering, Hakim Sabzevari University, Sabzevar, Iran

[2] Physiology and Pharmacology Department, Pasteur Institute of Iran, Tehran, Iran

[3] Department of Biomedical Engineering, Mashhad Branch, Islamic Azad University, Mashhad, Iran

recording and checking data extremely demanding time-consuming (Adeli et al. 2003; Tanq and Durand 2012). Therefore, automatic seizure detection is valuable for aiding neurologists to inspect EEG recordings. Accurate detection of seizures can be used to improve the diagnostic yield during patient monitoring for epilepsy surgery evaluation and to improve understanding of epilepsy as a dynamical disease. Additionally, automatic seizure detection can be used in automated closed-loop therapy, in which a therapy such as electrical stimulation, drug infusion, cooling, or biofeedback may be delivered in response to a seizure detection. The most important advantage of closed-loop therapy is that, the therapy can be utilized only when and where needed (Ramgopal et al. 2014).

Recently, several attempts have been reported for automatic detection of epileptic seizures by using EEG analysis. Gotman is one of the pioneers of automatic seizure detection whose research in this area dates back to 1976. Gotman and Gloor (1976) proposed a system for automatic detection of the interictal interval in EEG recordings using a spike and sharp wave recognition method. Adeli et al. (2007) proposed a method based on the nonlinear dynamics analysis of the EEG signal and its subbands. They classified the EEG signals into healthy, interictal and ictal. Polat and Günes (2007) used the power spectrum density (PSD) features to discriminate the healthy and ictal EEGs and achieved an accuracy of 98.72%. Kabir et al. (2018) used the combination of the K-mean clustering method with the support vector machine classifier and they could obtain an accuracy of 100% for seizure detection. Siuly et al. (2015) proposed a structure based on samplings and machine learning techniques for seizure detection and they could obtain an accuracy of 100%. Cumulants and higher order spectral features (Acharya et al. 2011; Mohsini et al. 2017; Chua et al. 2011; Srinivas et al. 2018), a series of entropies (Nicolaou and Georgiou 2012; Xiang et al. 2015; Srinivasan et al. 2007; Zhu et al. 2013) and Recurrence plot features (Acharya et al. 2011; Yan et al. 2016) were widely applied in epileptic seizure detection.

Recently, the combination of time series analysis and graph theory has created a new powerful nonlinear approach without the main deficiencies of common methods of time series processing (Donner et al. 2011; Nunez et al. 2012). In one simple approach, called visibility graph (VG), a time series is converted into a graph, the structure of which is proved to be related to complexity and fractality of the time series (Lacasa et al. 2008).

Some researchers have obtained promising results using VG methods, for the analysis of biological signals, such as EEG and electrocardiogram (ECG) (Ahmadlou et al. 2010; Nasrolahzadeh et al. 2019; Supriya et al. 2016).

Recently, VG methods have been used with promising results for automatic epileptic seizure detection. Tang et al. (Supriya et al. 2016) analyzed natural VG (NVG) from higher band frequencies of seizure EEGs and showed that the performance of the VG based approach is better than that of the simple entropy method in seizure detection. Zhu et al. (Tang et al. 2013) also extracted VG-based features to identify the ictal EEGs from healthy EEGs with 100% accuracy. Zhu et al. (Zhu et al. 2012) proposed a fast weighted horizontal VG (FWHVG) with an accuracy index of 100% for the discrimination of ictal from healthy EEG. In our previous work (Mohammadpoory et al. 2017), a weighted VG entropy (WVGE) was proposed and an accuracy index of 97% was obtained for discrimination of ictal, interictal and healthy groups.

In all previous studies, NVG and HVG methods have been used with a few numbers of graph properties. However, in the present study, all VG based methods were used with 14 number of graph properties as features used for the automatic detection of epileptic seizures in the epileptic rats.

Experimental animal models were widely used (Dedeurwaerdere 2005) to obtain greater insight into the pathophysiology underlying epilepsy. The most popular and widely used models are the subcutaneous (s.c.) pentylenetetrazole (PTZ) test and the maximal electroshock seizure test (Loscher and Schmidt 1988; Feltane et al. 2013; Sherman et al. 2011; Mirski et al. 2003; Kliouneva et al. 2001). These two seizure models have been implemented as a basis to develop various new antiepileptic drugs. Moreover, the s.c. PTZ test has been used to develop medications effective against generalized absence seizures (Loscher and Schmidt 1988). Töllner et al. (2016) compared the effects of five antiepileptic drugs on the PTZ seizure threshold in rats. Similarly, Moxon et al. (Moxon et al. 2001) used seizure-triggered trigeminal nerve stimulation in order to reduce PTZ-induced seizure activity in awakened rats. In another similar study, single and multiple stimulations were performed to examine the feasibility of an automatic seizure control system in rats with PTZ-induced seizures (Makeyev et al. 2012). However, an automatic seizure detector is needed before the application of the stimulation. So far, a variety of algorithms have been suggested for the detection of PTZ-induced seizures. For example, Besio et al. (2011) suggested a cumulative sum algorithm for the detection of such seizures. The detection accuracy index was then improved by combining this feature with the general likelihood ratio test (Makeyev et al. 2012). Moreover, Niknazar et al. (2013) proposed two approaches, thresholding, and classification, with several features for the detection of epileptic seizures in the epileptic rats.

There are some other features used for PTZ-induced seizure detection including cross-correlation variance (Makeyev et al. 2012) and cross-bicoherence gain

(Sherman et al. 2011). In addition to ECoG, optical coherence tomography (OCT) (Harreby et al. 2011), Laplacian EEG (Feltane et al. 2013) and vaguselectroneurogram (VENG) (Makeyev et al. 2012) were also implemented for the detection of PTZ-induced seizures in rats.

The purpose of the present study is to detect clonic seizures induced by injection of PTZ in rats, using VG based methods.

The rest of this paper is organized as follows: the experimental data are presented in the next section. Next, the methods and the quantification analyses used in the study are presented in "Methodology" section. The simulation results, the evaluation of the performance of the proposed method, and the discussions are summarized in "Results" and "Discussion" sections respectively. Finally, the conclusions are provided in "Conclusion" section.

Materials used

Dataset

The necessary data for the present study were collected at Pasteur Institute of Iran from male Wistar rats weighing 200–250 g. Having free access to food and water, the rats were kept in a controlled environment (6 am/6 pm light/-dark cycle; 22 ± 1 °C). Under ketamine (60 mg/kg, i.p.) and xylazine (10 mg/kg, i.p.) anesthesia, the rats received two screw electrodes inserted into their skull over the frontal and occipital cortex. Moreover, a dental acrrylic and an extra screw were used to fix the epidural electrodes on the skull. The rats were given a period of 3 days for recovery and were handled gently so that they could adapt with the recording procedure. Then, the ECoG was recorded in the control group for 60 min. For the experimental group, the ECoG signal was recorded a few minutes before the administration of a convulsive dose of pentylenetetrazole (60 mg/kg). While the rats were freely moving through a polyethylene tube, PTZ was injected s.c. to them. Next, the electrical activity was then recorded for 60 min. All the measurements and injections were performed between 10:00 and 15:00 h. Moreover, an AC differential amplifier (DAM 80,WPI) with a gain of 1000 and wiThe necessary data for the present study were collected at Pasteur Institute of Iran from male Wistar rats weighing 200–250 g. Having free access to food and water, the rats were kept in a controlled environment (6 am/6 pm light/-dark cycle; 22 ± 1 °C). Under ketamine (60 mg/kg, i.p.) and xylazine (10 mg/kg, i.p.) anesthesia, the rats received two screw electrodes inserted into their skull over the frontal and occipital cortex. Moreover, a dental acrrylic and an extra screw were used to fix the epidural electrodes on the skull. The rats were given a period of 3 days for recovery, and were handled gently so that they could adapt with the recording procedure. Then, the ECoG was recorded in the control group for 60 min. For the experimental group, the ECoG signal was recorded a few minutes before the administration of a convulsive dose of pentylenetetrazole (60 mg/kg). While the rats were freely moving through a polyethylene tube, PTZ was injected s.c. to them. Next, the electrical activity was then recorded for 60 min. All the measurements and injections were performed between 10:00 and 15:00 h. Moreover, an AC differential amplifier (DAM 80,WPI) with a gain of 1000 and with a band-pass filter setting of 0.1–1000 Hz was used to boost the ECoG signals. The sampling rate was 10 kHz, and the analog-to-digital conversion was performed at 12-bit resolution. The dataset for the final analysis were collected from 12 rats in the test group and 15 rats in the control group. The data of 6 rats in the test group had some issues due to sudden rat movements, amplifier saturation, and severe noise in data acquisition system. Therefore, some parts of the starting segments or ending segments of data from these 6 rats have been removed. However, remaining signals of these six rats were continuous.

A band-pass filter setting of 0.1–1000 Hz was used to boost the ECoG signals. The sampling rate was 10 kHz, and the analog-to-digital conversion was performed at 12-bit resolution. The dataset for the final analysis was collected from 12 rats in the test group and 15 rats in the control group.

An experienced experimental scientist observed animal behavior including head nodding and general clonus of the body (Danober et al. 1998), which corresponded to the score of 3 (myoclonic jerk) by Racine's seizures coring system (Racine 1972) in order to determine the seizure onset in each experiment. It was observed that PTZ initially produced myoclonic jerks, which subsequently became sustained, leading to generalized tonic–clonic seizures (De Deyn et al. 1992). However, the rats showed normal behavior again after some minutes, with no behavioral signs of the Racine scale. The return to normal behavior

Table 1 The time recording of each experiment

Rat no.	Injection time	Seizure onset	Seizure end
1	21:34	29:02	30:35
2	10:33	3:09	16:24
3	6:05	9:18	9:36
4	7:16	20:05	20:36
5	5:55	21:25	22:39
6	5:11	9:59	11:01

The time format is minute: second Starting time is always from 00:00

was considered as an indication of the end of the seizure. Table 1 summarizes data related to the injection time, seizure onset time and seizure end time of experiments for unsheared data.

Methodology

Preprocessing

At first, he ECoG signals were down sampled to 1 kHz, and filtered using a 50-Hz notch filter and a 60-Hz low pass filter. However, the collected data from 6 rats in the test group were problematic because of either sudden rat movements, amplifier saturation, or severe noise caused by the data collection procedures. As a result, the problematic parts of the starting segments or ending segments were eliminated from the final dataset. Apart from these problematic parts, in the remaining parts of the data related to these 6 rats, the signals were continuous. In other words, the excluded segments were always at the beginning or the end of the signals, not in the middle of them.

Feature extraction

The primary purpose behind feature extraction was to introduce the salient features discriminating seizure periods from seizure-free periods. In this study, five different VG based methods were constructed, with 14 graph properties extracted from these VGs, used as a basis to classify the two mentioned groups. All of the five VG based methods used along with the 14 features are described in the next sections.

Visibility Graph algorithms

Natural visibility algorithm

Let $\{x(t_i)\}i = 1 \ldots N$ be a time series of N data. The natural visibility algorithm (NVG) (Lacasa et al. 2008) maps every datum of the time series on to a node in the graph. Two nodes i and j in the graph are connected if one can draw a straight line in the time series connecting $x(t_i)$ and $x(t_j)$, cutting no intermediate data $x(t_k)$. Hence, i and j are two connected nodes if:

$$x(t_k) < x(t_i) + (x(t_i) - x(t_i))\frac{t_k - t_i}{t_j - t_k} \quad (1)$$

Figure 1 shows a graphical illustration of the construction of NVG from a time series. This algorithm constructs regular graphs from periodic time series, random graphs from random time series, and scale-free graphs from fractal time series. Some important properties of these graphs can be found in (Ni et al. 2009; Lacasa et al. 2009).

Horizontal visibility algorithm

A horizontal visibility graph (HVG) was proposed by Luque et al. (2009). In HVG, like NVG, every point of the time series maps onto a node in the graph. Two nodes i and j in the graph are connected if and only if:

$$x_i > x_k \text{ and } x_j > x_k; \text{ for all k such that } i < k < j \quad (2)$$

Figure 2 shows an illustration of the construction of HVG from a time series. This algorithm is a simplification of the NVG. In fact, the HVG is always a sub-graph of its associated NVG for the same time series (comparing Figs. 1 and 2). Some concrete properties of these graphs can be found in (Lacasa and Toral 2010; Lacasa et al. 2012; Luque et al. 2011; Gutin et al. 2011).

Limited penetrable visibility graph (LPVG)

Based on NVG, Ting–Ting et al. (Zhou et al. 2012) presented LPVG and showed that LPVG has an advantage over NVG in that it enjoys a good tolerance to noise. Like NVG, every point in the series corresponds to a node in the graph, such that two nodes are connected if the straight line connecting the series data intersects intermediate data height in maximum N points. NVG is a simplification of the LPVG algorithm when N = 0. Figure 3 shows LPVG construction from a time series (N = 1).

Parametric natural visibility graph (PNVG)

Based on NVG, Bezsudnov and Snarskii (2014) presented PNVG and showed that the PNVG approach allows us to distinguish, identify and describe various time series in detail. The PNVG algorithm consists of three main steps: first, the NVG (Lacasa et al. 2008) is built. Then, the temporal direction is added to every NVG link, and the weight equal to the angle between the link and the downward directions is set. The weight value between the two nodes is defined as follows:

$$\alpha_{ij} = \frac{x(t_j) - x(t_i)}{t_j - t_i} \quad i < j \quad (3)$$

Finally, PNVG is constructed from NVG links which have weights less than the given view angle α (α is an arbitrary changing parameter). PNVG is a directed sub-graph of the corresponding NVG, and not necessarily a connected graph. Figure 4 shows the construction of the PNVG from a time series.

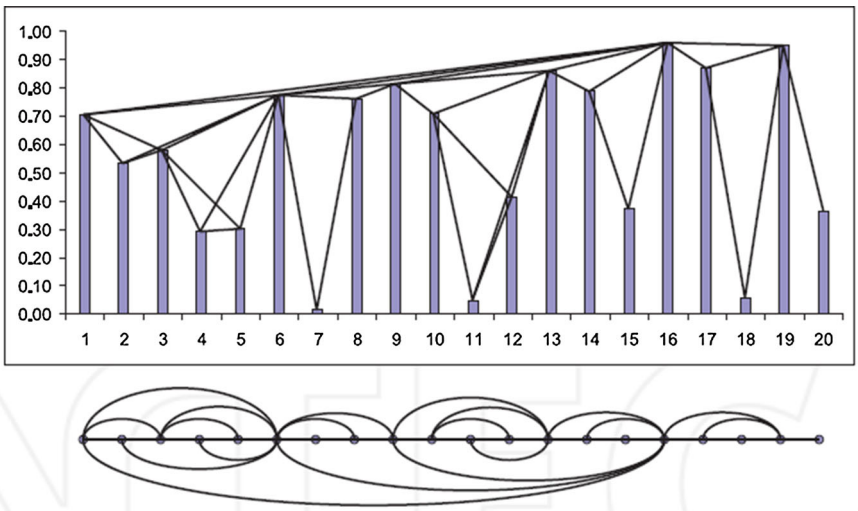

Fig. 1 An example of the NVG construction. The upper part shows time series and lower part represents the NVG (Lacasa et al. 2008)

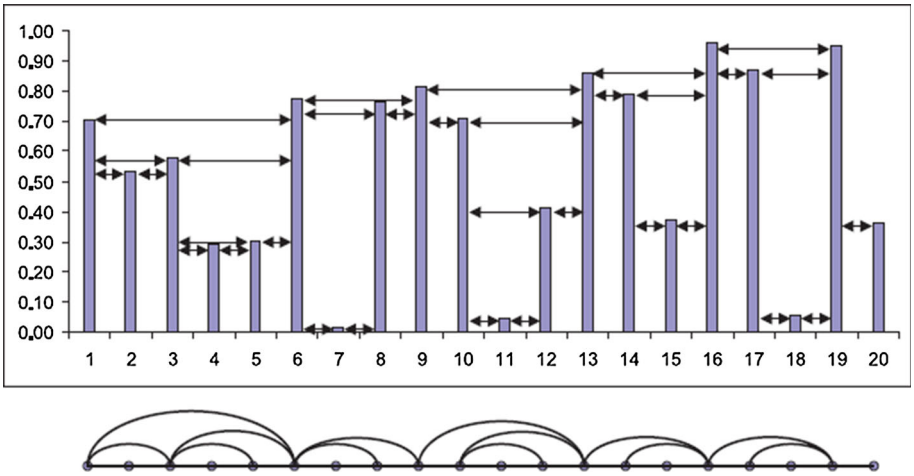

Fig. 2 An example of the HVG construction. The upper part shows time series and lower part represents the HVG (Luque et al. 2009)

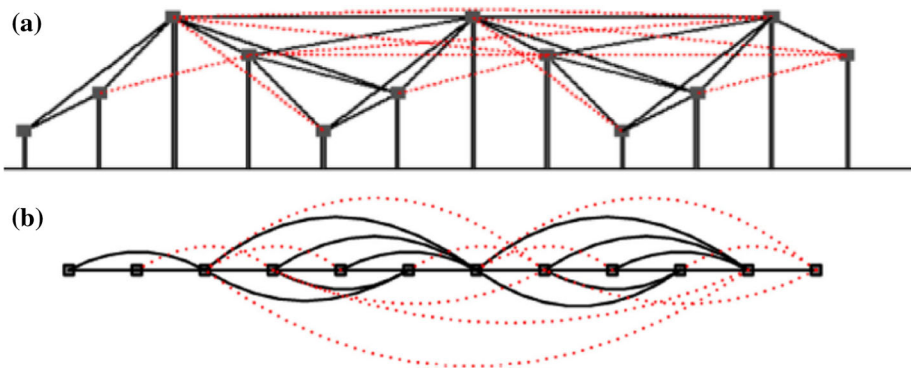

Fig. 3 Illustrates the procedure of converting time series to the LPVG (N = 1). **a** Time series: each black line shows the two connected points can see each other. The red lines are extra connections in LPVG compared with VG. **b** Corresponding graph: The LPVG consists of red and black links and the NVG consists only of black links (Pei et al. 2014). (Color figure online)

Markov-binary visibility graph (MBVG)

Ahadpour et al. (Ahadpour et al. 2014) presented MBVG using a two-state Markov chain and the binary visibility graph for investigation of time series. Let $\{x(t_i)\}i = 1 \ldots N$ be a time series of N data. Then, we consider slope (m) between any two consecutive data in the time series

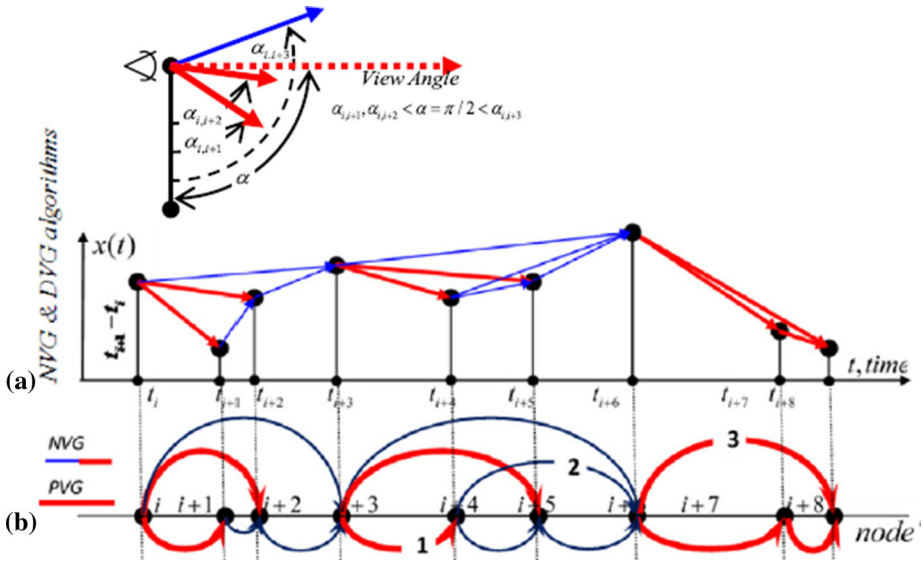

Fig. 4 The Illustration of the PNVG algorithm. **a** Time series plot for NVG and PNVG algorithms, **b** corresponding graphs, The NVG consists of red and blue links. The PNVG ($\pi/2$) consists only of red links. Upper left—the PNVG link selection criterion for view angle $\alpha = \pi/2$ applied to nodes (t_i) (Bezsudnov and Snarskii 2014). (Color figure online)

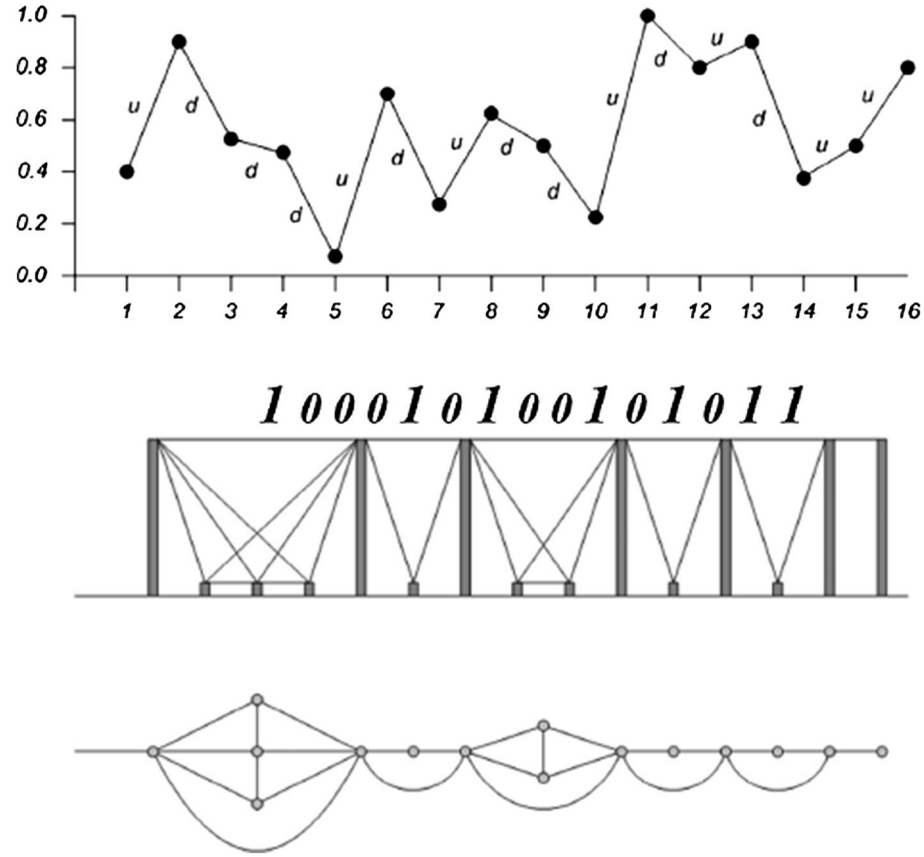

Fig. 5 An example of the Markov-binary visibility graph construction. The upper part shows time series and intermediate part shows the Markov binary sequence generated from time series. The bottom part represents the graph generated through the visibility algorithm (Ahadpour et al. 2014)

line diagram (see Fig. 5). Then, a two-state Markov chain of states 0 and 1is defined as follows

For the stochastic systems,

$$S = \begin{cases} 0 & m \leq 0 \\ 1 & m > 0 \end{cases} \tag{4}$$

and for the deterministic systems,

$$S = \begin{cases} 0 & m \geq 0 \\ 1 & m < 0 \end{cases} \tag{5}$$

The Markov-binary visibility algorithm assigns every bit of the sequence to a node in the MBVG. Two nodes i and j in the MBVG are connected with the criteria of the NVG.

Graph properties

After graphs are constructed from data, some measures are estimated for the analysis of graph structure and topology to discriminate two groups of seizure and seizure free signals. All these measures are defined for binary graphs. Since LPVG is a weighted and directed graph, these measures are defined in different way for it, and for further information see ref (Rubinov and Sporns 2010).

Assume that K = k(i), i = 1,…, N (N is the number of nodes in VG) is the degree sequence (DS) of VG (the degree of a node is the number of edges incident to the vertex) and $A = [a_{ij}]_{N\times N}$ is the adjacency matrix of VG in which $a_{ij} = 1$, if node i is connected to node j and $a_{ij} = 0$ if node i is not connected to node j. The extracted VG based features are:

1. Mode of the DS values (M1).
2. Mean of the DS values (M2).
3. Median of the DS values (M3).
4. Maximum of the DS values (M4).
5. Minimum of the DS values (M5).
6. Maximum of the DS values divided by Median of the DS values (M6).
7. The standard deviation of the DS values (S).
8. Number of the nodes having the DS mode value multiplied by the DS mode value divided by the sum (K).
9. Graph index complexity: Let kmax be the largest eigenvalue of the adjacency matrix. GIC is defined as (Kim and Wilhelm 2008):

$$IGIC = 4C(1 - C), \tag{6}$$

where

$$C = \frac{kmax - 2\cos(\pi/N + 1)}{N - 1 - 2\cos(\pi/N + 1)}, \tag{7}$$

10. Characteristic path length (del Sol et al. 2006) (L): The characteristic path length (L) of a graph is the shortest path length between two nodes averaged over all nodes and is given by:

$$L = \frac{\sum_i \sum_j L_{ij}}{N(N-1)}, \tag{8}$$

where L_{ij} is the shortest path length between ith node and jth node and N is the total number of nodes in the network.

11. Global efficiency (Wang et al. 2010) (Eg): The global efficiency is defined as:

$$Eglob = \frac{1}{N(N-1)} \sum_{i\neq j} \frac{1}{d_{ij}}, \tag{9}$$

where d_{ij} is the shortest path length between node I and *node* j *in* graph.

12. Average clustering coefficient (Lenjani and Hashemi 2014) (CL): The clustering coefficient (cl_i) of a node, in a graph is given by:

$$cl_i = \frac{2e_i}{K_i(K_i - 1)}, \tag{10}$$

where e_i is the total number of the edges really connecting its nearest neighbors to the ith node and K_i is the degree of the ith node. The average clustering coefficient of a network is given by

$$CL = \frac{\sum_i cl_i}{N}, \tag{11}$$

13. Local efficiency (Wang et al. 2010) (El): The local efficiency is measured as

$$Eloc = \frac{1}{N} \sum_i Eglob(G_i), \tag{12}$$

where $Eglob(G_i)$ is the global efficiency of G_i, the sub-graph composed of the neighbors of node i.

14. Assortative coefficient (Lenjani and Hashemi 2009): Assortativity, is a preference for a graph's nodes to attach to similar nodes in some way. Network theorists often estimate assortativity in terms of a node's degree. The assortative property of a network is defined by the assortative coefficient. The assortative coefficient is defined as:

$$r = \frac{M^{-1}\sum_i j_i k_i - \left[M^{-1}\sum_i 0.5(j_i + k_i)\right]^2}{M^{-1}\sum_i 0.5(k_i^2 + j_i^2) - \left[M^{-1}\sum_i 0.5(j_i + k_i)\right]}, \tag{13}$$

where k_i and j_i are the degree of two nodes at the ends of the ith link, and M is the number of total links.

All of these features were estimated using the Matlab software.

Feature selection algorithm

Because the reduction of data generally leads to an improvement in the classification performance in terms of speed, accuracy and simplicity, the feature selection has been used extensively to reduce the data dimensionality (Schenk et al. 2009). The sequential search algorithms have attracted extensive attention as a strategy to reduce the number of features in local search.

In this paper, a feature selection method based on Sequential Forward Selection (SFS) was implemented to estimate the prediction error as a selection criterion. Generally speaking, sequential search algorithms are strategies

that reduce the number of features applying local search (Kudo and Sklansky 2000). The SFS method begins with a set of features and a sequential way adding parameters, continuing until the criterion of selection has reached a minimum, or all the parameters are added to the model.

Note that SFS is a bottom-up search procedure starting from an empty feature set S and gradually adding features selected by some evaluation functions, that minimizes the mean square error (MSE) (Last et al. 2001). At each iteration, the feature to be included in the feature set is selected from among the remaining available features of the feature set not added to the feature set. Therefore, the new extended feature set should produce a minimum classification error compared with when any other feature is added. Because of its important characteristics including simplicity and speed, SFS have been widely used in a variety of areas (Nakariyakul and Casasent 2009; Muni et al. 2006).

Classification method

The application of classifiers in medical diagnosis has increased recently (Siuly et al. 2016). Artificial Neural Networks (ANNs) are computing systems made up of a large number of simple interconnected processing elements called neurons. They have been widely used as classifiers in diagnostic systems, and as a basis for the analysis of biological signals (Siuly et al. 2016; Vieira et al. 2013). The results of the studies reported in the literature show that ANNs have always been a good classifier in detecting epileptic seizures (Asadi et al. 2015; Kelwade and Salankar 2016). In the present study, a multilayer perceptron (MLP) neural networks classifier was used. Note that the network structure directly influences the performance of the classifier. After an appropriate structure and a suitable number of training epochs were found with the aim of validating the set, the testing patterns were utilized for the evaluation of the performance of the proposed method. ANN toolbox of MATLAB software was used to run the MLP.

Results

Figure 6 summarizes the long-term ECoG recordings of a rat in the test group. The seizure interval is shown in this figure. For the experiments, the first 5 min from each recorded signal are considered as seizure-free data. Then seizure and seizure-free intervals of ECoG signals were divided into equal epochs. According to Tang et al. (Supriya et al. 2016), there is no point in using a large number of data for the conversion of EEG signal into the graph because the quantification of self- similarity and complexity of a graph does not need many nodes. The amount of data can be increased through the segmentation of a signal as a part of the entire dataset in that it provides more meaningful information (Supriya et al. 2016). However, Supriya et al. (Zhu et al. 2014) showed that the use of segmented versus non-segmented approaches for EEG signals leads to no significant difference in the performance accuracy index obtained although the segmentation of EEG signals makes the computation faster. Therefore, in the present study, 1000 (1 s) and 2000 (2 s) data point epochs were used in the analyses in that longer epochs make the calculation process very tedious and time-consuming. In the case of 1000 point epoch, 3600 seizure-free and 720 seizure epochs, and in the case of 2000 point epoch, 1800 seizure-free and 360 seizure epochs were obtained.

Then, five VGs were constructed for all the epochs from the two sets, then the 14 explained features were extracted from these graphs. Next, a sequential forward feature selection algorithm was used to select the most informative features which were then fed into MLP classifier for the discrimination of the two groups. In this study, 60% of the input patterns were assigned to the training set, 20% of them were assigned to the validation set, while the remaining 20% were assigned to the testing set. Since the number of seizure-free epochs were much higher than the seizure epochs, and because classifiers usually tend to obtain higher accuracy indexes for classes with more training samples, the number of seizure-free samples of the training set were reduced by re-sampling so that a balanced number of samples for the two classes could be attained (Chawla et al. 2004).

In order to find the suitable structure of the MLP, the number of hidden layers and their nodes were being changed until the best network structure was obtained. On the other hand, the accuracy index for validation set was calculated in every 1000 training epochs so that the appropriate structure could be found while over-training could be avoided. In this study, the sigmoid function and a linear activation function were applied as the activation functions of all internal nodes and the output node, respectively.

After an appropriate structure was found, the testing patterns were utilized for the evaluation of the performance of the proposed method. In the present study, some statistical parameters such as sensitivity, specificity, and total classification accuracy were used as bases for the evaluation of the performance reliability of the classifier. These parameters were defined as follows (Nasrolahzadeh et al. 2015):

Sensitivity: number of true positive decisions/number of actually positive cases.

Specificity: number of true negative decisions/number of actually negative cases.

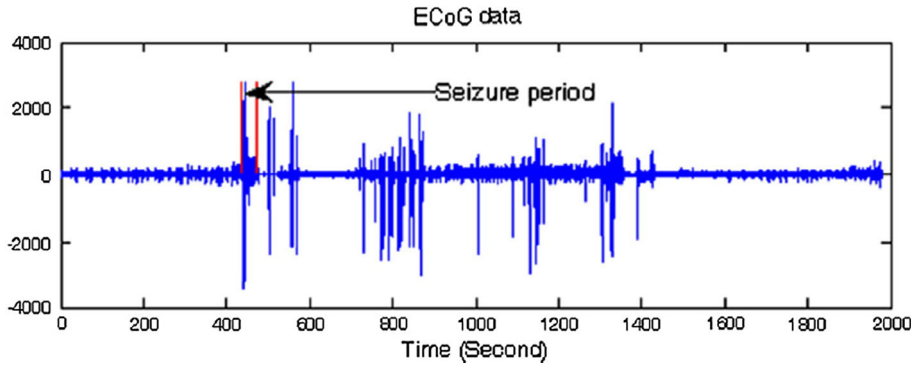

Fig. 6 The long-term ECoG recordings of a rat in the test group. Seizure interval is indicated in this Figure

Total classification accuracy: number of correct decisions/total number of cases.

Tables 2 and 3 present the classification results obtained using five different VG methods and two different lengths of epochs. For LPVG, it was assumed that N = 1 and N = 2 because research studies done so far have shown that the proper amounts of N are 1 and 2 (Zhou et al. 2012). For PNVG, it is assumed that $\alpha = \pi/4$, $3\pi/8$, and $\pi/2$. The Results showed that all of the methods enjoyed acceptable accuracies and high sensitivity indexes. The best accuracy was obtained by the LPVG (N = 2 and epoch length = 2000) while the worst obtained by the HVG (epoch length = 1000).Since the LPVG methods were more robust to noise than the others (Zhou et al. 2012) and ECoG signal was very noisy, especially in the seizure state, this method performed better than the others. Also, longer epoch leads to better accuracies in most of VG based methods, but more calculations are required. Therefore, the speeds of the algorithms for different lengths of epochs were compared.

Table 4 shows the average time cost in seconds for the calculation of 14 features of eight VG based methods and the two different lengths of epochs. All algorithms were run on a 2.4 GHz Intel core i5 CPU processor machine with4 GB RAM. The operating system was Windows 7 and 64 bits. As can be seen, the PNVG ($\alpha = \pi/4$) and the HVG had the highest speed indexes because of their sparse adjacency matrixes. But the MBVG had the lowest speed because, after mapping the time series on the 0 and 1 sequence, the number of visibility links was much higher than that of the visibility links obtained via original time series, and thus the adjacency matrix became denser.

Table 3 The values of statistical parameters for different VG methods and epoch length of 2000

Statistical parameters (%) VG method	Sensitivity	Specificity	Accuracy
NVG	96.53	80.94	89.01
HVG	85.96	57.1	71.54
MBVG	96.51	80.22	89.64
LPVG (N = 1)	95.81	76.87	87.19
LPVG (N = 2)	98.94	86.03	92.13
PNVG ($\alpha = \pi/4$)	83.45	55.02	70.21
PNVG ($\alpha = 3\pi/8$)	92.24	71.98	81.41
PNVG ($\alpha = \pi/2$)	91.54	68.69	76.25

Table 2 The values of statistical parameters for different VG methods and epoch length of 1000

Statistical parameters (%) VG method	Sensitivity	Specificity	Accuracy
NVG	95.41	75	85.88
HVG	81.94	54.16	68.54
MBVG	9.32	76.85	84.64
LPVG (N = 1)	96.81	81.97	89.19
LPVG (N = 2)	98.31	84.83	91.54
PNVG ($\alpha = \pi/4$)	87.3	66.52	76.71
PNVG ($\alpha = 3\pi/8$)	88.11	68.18	77.41
PNVG ($\alpha = \pi/2$)	85.93	61.02	74.25

Table 4 The average time costing in second of14 VG based measures calculation foreight VG methods and two different lengths of epochs

Epoch size VG method	1000	2000
NVG	15.17	42.48
HVG	2.86	5.14
MBVG	75.12	542.32
LPVG (N = 1)	25.42	52.14
LPVG (N = 2)	64.32	148.56
PNVG ($\alpha = \pi/4$)	2.45	4.06
PNVG ($\alpha = 3\pi/8$)	3.39	5.78
PNVG($\alpha = \pi/2$)	3.97	6.45

Considering both the speed and accuracy, LPVG and NVG showed promising results. The PNVGs were fast, enjoying relatively good accuracy indexes. Although the HVG was equally fast, it suffered the lowest accuracy index. Conversely, MBVG had a relatively good accuracy but it was very slow. As can be seen, the different methods had different accuracies and speeds, thus the selection of one over another is a function of the relative importance of accuracy or speed in a given application.

Since different studies used different databases and study populations, different number of classes (two, three, four or five classes), different classifiers and common types of cross-validation approaches (K-fold or leave-one-out cross-validation), no cross comparison among them was possible. Therefore, in this study, several methods of signal processing were implemented for seizure detection. The Largest Lyapunov exponent (LLE), Fractal dimension (FD) and bispectrum based features (BIS) were used as nonlinear features. Details of these methods are presented in "Appendix".

Table 5 shows classification results obtained using three mentioned methods and LPVG (N = 2) method. As shown, the proposed method performs better than three other methods.

Our proposed method was also applied to the recorded EEG signals from Bonn (http://www.meb.uni-bonn.de/epileptology/science/physik/eeg.data.html) database to show the efficiency of the proposed method for human seizure detection. Sets Z (healthy) and S (seizure) from this online EEG dataset were selected to test the method proposed for seizure detection. The database was analyzed under the same experimental conditions, and with the same procedure. Tables 6 presents accuracies obtained using five different VG methods and two different lengths of epochs. As can be seen, proposed method can detect seizure with high accuracy of 100%.

Table 5 The values of statistical parameters for the LLE, FD, BIS and LPVG (N = 2) methods

Statistical parameters (%) VG method	Sensitivity	Specificity	Accuracy
LLE	83.25	61.47	70.65
FD	79.84	55.48	68.45
BIS	95.23	79.57	87.32
LPVG (N = 2)	98.94	86.03	92.13

Table 6 The classification accuracies for different VG methods and four different lengths of epochs for human database

Epoch size VG method	1000	2000
NVG	100	100
HVG	92.31	91.57
MBVG	95.45	98.54
LPVG (N = 1)	100	100
LPVG (N = 2)	100	100
PNVG ($\alpha = \pi/4$)	93.52	94.25
PNVG ($\alpha = 3\pi/8$)	97.3	95.24
PNVG ($\alpha = \pi/2$)	96.87	97.46

Discussion

This paper presented an innovative method for detection of seizures in epileptic rats, based on five VG-based algorithms and 14 graph properties with MLP classifier. The studies proposing the use of NVG and HVG methods for seizure detection validated their proposed methods on human database.

To the best knowledge of the authors, the VG based methods have never been applied for automatic seizure detection in animals. Also, neither LPVG, PNVG and, MBVG algorithms nor, GIC, Eg, r, El, C, L and, K features have been used in the automatic seizure detection methods. Tables 2 and 3 show that compared to other methods, the LPVG method had the highest accuracy index along with a reasonable speed index. This study also investigated the effect of epoch size on performance, showing that although longer epochs led to better accuracies, they made the analyses more time-consuming.

In the literature, two approaches were proposed for the detection of seizure: thresholding and classification. In the former approach, a feature is calculated in consecutive windows, with the resulted index being tracked over time and compared with a threshold. In this approach, the seizure onset is considered the moment the index crosses the threshold. In the classification approach, however, features from seizure and seizure-free periods are extracted and statistically analyzed. There are significant differences in the statistical characteristics of some features in these periods, which can serve as a basis for the detection of epileptic seizure. Some researchers have used classification methods to distinguish seizure from seizure-free periods, using these extracted features. In the first approach, just one feature can be used for seizure detection while, in the other, it is possible to use more than one feature. In this study, the second approach was followed for seizure detection, and the proposed method was proved successful

and effective in seizure detection. Several researchers have used the second approach for automatic seizure detection in rats, obtaining good results. Bergstrom et al. (Bergstrom et al. 2013) proposed Spike detection using total signal variation and wavelet decomposition to detect seizures in epileptic rats. They used 36 channels ECoG signals and obtained a high accuracy index of 99%.

Buteneers et al. (2011) used the following features: a filter bank of Butterworth filters ranging from 1 to 30 Hz with a bandwidth of 2 Hz, a set of Daubechies 4 wavelet filters (levels 2–6), the first derivative, the energy of the signal and the energy in the theta, alpha, beta and gamma bands with reservoir computing (RC) classification algorithm. They have evaluated their method on data containing two different seizure types: absence seizures from genetic absence epilepsy rats from Strasbourg (GAERS) and tonic–clonic seizures from kainate-induced temporal-lobe epilepsy rats. Using the one channel ECoG signal, this method resulted in a sensitivity index of 96% and 94% and a specificity index of 96% and 99% on the data from GAERS and kainate rats, respectively.

Makeyev et al. (Besio et al. 2011) proposed the combination of detections from a cumulative sum algorithm and a generalized likelihood ratio test to analyze Laplacian electroencephalography (tEEG) signals. An average seizure onset detection accuracy of 76.14% was obtained.

Feltane et al. (2013) proposed three features, namely, median absolute deviation, approximate entropy and maximum singular value to be calculated from tEEG data, and be fed as inputs into two different classifiers: support vector machines and adaptive boosting. The results showed an overall accuracy between 84.81 and 96.51%.

The main advantage of the present model is that 14 features were examined. Most of the previous studies in the area of PTZ-induced seizure detection employed only one, two or three features. Applying a wide range of features with different levels of complexity and sensitivity can reveal suitability of each feature for the detection of PTZ-induced seizures. Moreover, the present study included more rats in its dataset compared to the majority of the studies done so far (Feltane et al. 2013; Sherman et al. 2011; Moxon et al. 2001; Makeyev et al. 2012; Harreby et al. 2011; Paul et al. 2003; Fanselow et al. 2000).

Further, the proposed method for detecting seizure segments was robust; it enjoyed a high accuracy index even though the data were contaminated with artifacts.

In the future studies, we intend to propose a new method for transforming time series into the graph for faster and more accurate epileptic seizure detection.

Conclusion

In this study, an approach based on the transformation of time series onto graph was used for the detection of induced epileptic seizures. In this study, seizures were induced in rats using the PTZ model, and ECoG signals were analyzed. For this purpose, five algorithms for transforming of time series into complex networks, i.e., NVG, HVG, PNVG, LPVG and, MBVG, were used. Moreover, VG based methods were used for the first time for the analysis of ECoG signals in rats. In addition, for the first time, LPVG, PNVG and, MBVG along with a number of graph properties namely GIC, Eg, r, El, C, L and, K were successfully employed to detect seizures. The highest accuracy index was obtained by the LPVG method with N = 2 and an epoch length of 2000 data points. Furthermore, it was shown this method was highly robust in detecting seizure segments; it achieved a high accuracy index even though the data were contaminated with artifacts. Results show, the proposed method has also better performance comparing to some other methods. Therefore, the proposed method was shown to be accurate, robust, and fast, and can be used for real-time seizure detection.

Appendix

Fractal dimension, largest Lyapunove exponent and Bispectrum

In this section, three methods used in work are briefly introduced.

1. FD: fractal systems have self-similarity characteristic. Self-similarity can be measured by the number of basic building units that form a pattern, and this measure is defined as the FD. Several algorithms have been proposed for FD estimation (Lacasa et al. 2009; Higuchi 1988; Katz 1988; Asvestas et al. 1999), and in this work Higuchi (Higuchi 1988) method were used.

2. LLE: LE is a measure of the exponential divergence/convergence of initially nearby trajectories in the phase space (Abarbanel et al. 1993). Since there was only time series, a pseudo phase space or Reconstructed Phase Space (RPS) of the system is constructed using Time Delay Embedding (TDE) method.

Suppose $\{x_i\}$ represents the time series. The RPS is created with a time delay τ and an embedding dimension m. The RPS matrix is formed as follows (Nasrolahzadeh et al. 2015):

$$\begin{bmatrix} x_0 & x_\tau & \cdots & x_{(n-1)\tau} \\ x_1 & x_{1+\tau} & \cdots & x_{1+(n-1)\tau} \\ x_2 & x_{2+\tau} & \cdots & x_{2+(n-1)\tau} \\ \vdots & \vdots & \vdots & \vdots \end{bmatrix}$$

Parameter τ can be obtained through a number of different methods. In this study, "finding of the mutual information function" method was used for estimation of τ.

After the optimal lag has been selected, the dimension (m) is estimated by Cao's method (Nasrolahzadeh et al. 2015).The number of Lyapunov exponents is equal to (that of) the embedding dimension of the attractor. For a system to have at least one positive LE (which implies that the largest Lyapanove exponent (LLE) is greater than zero) leads to be chaotic.

Consider two nearest neighboring points in the phase space at time 0 and t, the distances of the points in the ith direction from these points are shown by $\delta x_i(0)$ and $\delta x_i(t)$, respectively. The Lyapunov exponent is defined by the mean growth rate λ_i of the initial distance;

$$\frac{\delta x_i(t)}{\delta x_i(0)} = 2^{\lambda_i t}, \quad \forall t \to \infty, \tag{14}$$

$$\lambda_i = \lim_{t\to\infty} \frac{1}{t} \log_2 \frac{\delta x_i(t)}{\delta x_i(0)}, \tag{15}$$

Two general methods used for the calculation of the LE from time series are the geometrical and Jacobian approaches. In this paper, the first method was used. The first is based on following the time-evolution of nearby points in the phase space. This algorithm estimates the LLE only (Nasrolahzadeh et al. 2015).

3. BIS: BIS is the Fourier transform of the third order correlation of the time series and is defined as:

$$B(f_1,f_2) = E[X(f_1)X(f_2)X^*(f_1+f_2)], \tag{16}$$

where X is the Fourier transform of the signal x, X^* is the complex conjugate of X and E[] is an average over an ensemble of realizations of a random signal (Nasrolahzadeh et al. 2016).

Equation (16) shows the bispectrum is a function of two frequency variables and complex-valued.

Bispectrum can be estimated through various methods (Chua et al. 2009). In this paper, direct (FFT-based) (Nasrolahzadeh et al. 2018) is used to estimate Bispectrum.

The extracted bispectral based features in this study are:

1. Mean of bispectral magnitude:

$$M_{avg} = \frac{1}{L}\sum_{\Omega} |B(f_1,f_2)|, \tag{17}$$

where L is the number of points within the region Ω.

2. Max of bispectral magnitude within the region.

$$Max = \max_{\Omega} |B(f_1,f_2)|, \tag{18}$$

3. Min of bispectral magnitude within the region.

$$Min = \min_{\Omega} |B(f_1,f_2)|, \tag{19}$$

4. The sum of the logarithmic amplitudes of the bispectrum (Mookiah et al. 2012):

$$H = \sum_{\Omega} Log(|B(f_1,f_2)|), \tag{20}$$

5. Bispectral phase entropy (Ph) (Mookiah et al. 2012):

$$Min = \min_{\Omega} |B(f_1,f_2)|, \tag{21}$$

where

$$p(\psi_n) = \frac{1}{L}\sum_{\Omega} I(\phi(B(f_1,f_2)) \in \psi_n), \tag{22}$$

$$\psi_n = \left\{ \phi | -\pi + \frac{2\pi n}{N} \le \phi < -\pi + \frac{2\pi(n+1)}{N} \right\}, \tag{23}$$

n = 0, 1, …, N − 1where ϕ is the phase angle of the bispectrum, and I(.) is a function which obtains a value of 1 when ϕ is within the range bin ψ_n depicted by in Eq. (23).

6. Bispectrum entropies (Mookiah et al. 2012):

$$P_1 = -\sum_k p_k \log p_k, \tag{24}$$

where

$$p_k = \frac{|B(f_1,f_2)|}{\sum_\Omega |B(f_1,f_2)|}, \tag{25}$$

$$P_2 = -\sum_i q_i \log q_i, \tag{26}$$

where

$$q_i = \frac{|B(f_1,f_2)|^2}{\sum_\Omega |B(f_1,f_2)|^2}, \tag{27}$$

$$P_3 = -\sum_n r_n \log r_n, \tag{28}$$

where

$$r_n = \frac{|B(f_1,f_2)|^3}{\sum_\Omega |B(f_1,f_2)|^3}, \tag{29}$$

References

Abarbanel HDI, Brown R, Sidorowich JJ, Tsimring LS (1993) The analysis of observed chaotic data in physical systems. Rev Mod Phys 65:1331. https://doi.org/10.1103/RevModPhys.65.1331

Acharya UR, Sree SV, Suri JS (2011a) Automatic detection of epileptic EEG signals using higher ordercumulant features. Int J Neural Syst 21(5):403–414

Acharya UR, Sree SV, Chattopadhyay S, Yu W, Ang PC (2011b) Application of recurrence quantification analysis for the automated identification of epileptic EEG signals. Int J Neural Syst 21(3):199–211

Adeli H, Zhou Z, Dadmehr N (2003) Analysis of EEG records in an epileptic patient using wavelet transform. J Neurosci Methods 123(1):69–87

Adeli H, Ghosh-Dastidar S, Dadmehr N (2007) A wavelet-chaos methodology for analysis of EEGs and EEG subbands to detect seizure and epilepsy. IEEE Trans Biomed Eng 54(2):205–211

Ahadpour S, Sadra Y, ArastehFard Z (2014) Markov-binary visibility graph: a new method for analyzing complex systems. Inf Sci 274:286–302

Ahmadlou M, Adeli H, Adeli A (2010) New diagnostic EEG markers of the Alzheimer's disease using visibility graph. J Neural Transm 117(9):1099–1109

Asadi F, Mollakazemi MJ, Atyabi SA, Uzelac I, Ghaffari A (2015) Cardiac arrhythmia recognition with robust discrete wavelet-based and geometrical feature extraction via classifiers of SVM and MLP-BP and PNN neural networks. In: IEEE conference publications on 2015 computing in cardiology conference (CinC). https://doi.org/10.1109/cic.2015.7411065

Asvestas P, Matsopoulos GK, Nikita KS (1999) Estimation of fractal dimension of images using a fixed mass approach. Pattern Recognit Lett 20(3):347–354

Bergstrom RA, Choi JH, Manduca A, Shin HS, Worrell GA, Howe CL (2013) Automated identification of multiple seizure-related and interictalepileptiform event types in the EEG of mice. Sci Rep 3:1483

Besio WG, Liu X, Liu Y, Sun YL, Medvedev AV, Koka K (2011) Algorithm for automatic detection of pentylenetetrazole-induced seizures in rats. Conf Proc IEEE Eng Med Biol Soc 2011:8283–8286

Bezsudnov IV, Snarskii AA (2014) From the time series to the complex networks: the parametric natural visibility graph. Physica A 414:53–60

Buteneers P, Verstraetena D, van Mierlo P, Wyckhuys T, Stroobandt D, Raedt R, Hallez H, Schrauwena B (2011) Automatic detection of epileptic seizures on the intra-cranial electroencephalogram of rats using reservoir computing. Artif Intell Med 53(3):215–223

Chawla NV, Japkowicz N, Kotcz A (2004) Editorial: special issue on learning from imbalanced data sets. ACM SIGKDD Explor Newslett 6(1):1–6. https://doi.org/10.1145/1007730.1007733

Chua CK, Chandran V, Acharya RU, Mi LCh (2009) Cardiac health diagnosis using higher order spectra and support vector machine. Open Med Inform J 3:1–8

Chua KC, Chandran V, Acharya UR, Lim CM (2011) Application of higher order spectra to identify epileptic EEG. J Med Syst 35(6):1563–1571

Danober L, Deransart C, Depaulis A, Vergne M, Marescaux C (1998) Pathophysiological mechanisms of genetic absence epilepsy in the rat. Prog Neurobiol 55(1):27–57

De Deyn PP, D'Hooge R, Marescau B, Pei YQ (1992) Chemical models of epilepsy with some reference to their applicability in the development of anticonvulsants. Epilepsy Res 12(2):87–110

Dedeurwaerdere S (2005) Neuromodulation in experimental animal models of epilepsy. In: PhD thesis. Ghent University, Ghent

del Sol A, Fujihashi H, Amoros D, Nussinov R (2006) Residues crucial for maintaining short paths in network communication mediate signaling in proteins. Mol Syst Biol. https://doi.org/10.1038/msb4100063

Donner RV, Small M, Donges JF, Marwan N, Zou Y, Xiang R, Kurths J (2011) Recurrence-based time series analysis by means of complex network methods. Int J Bifurc Chaos 21(4):1019–1046

Fanselow EE, Reid AP, Nicolelis MA (2000) Reduction of pentylenetetrazole-induced seizure activity in awake rats by seizure-triggered trigeminal nerve stimulation. J Neurosci 20(21):8160–8168

Feltane A, Faye Boudreaux-Bartels G, Besio W (2013) Automatic seizure detection in rats using Laplacian EEG and verification with human seizure signals. Ann Biomed Eng 41(3):645–654

Firpi H, Goodman ED, Echuaz J (2007) Epileptic seizure detection using genetically programmed artificial features. IEEE Trans Biomed Eng 54(2):212–224

Gotman J, Gloor P (1976) Automatic recognition and quantification of interictal epileptic activity in the human scalp EEG. Electroencephalogr Clin Neurophysiol 41(5):513–529

Gutin G, Mansour T, Severini S (2011) A characterization of horizontal visibility graphs and combinatorics on words. Physica A 390(12):2421–2428

Harreby KR, Sevcencu C, Struijik JJ (2011) Early seizure detection in rats based on vagus nerve activity. Med Biol Eng Comput 49(2):143–151

Higuchi T (1988) Approach to an irregular time series on the basis of the fractal theory. Physica D 31(2):277–283

Institute of Medical Biometry, Informatics and Epidemiology of the "MedizinischeEinrichtungen der Universität Bonn": http://www.meb.uni-bonn.de/epileptology/science/physik/eeg.data.html

Kabir E, Siuly S, Cao J, Wang H (2018) A computer aided analysis scheme for detecting epileptic seizure from EEG data. Int J Comput Intell Syst 11(1):663–671

Katz MJ (1988) Fractals and the analysis of waveforms. Comput Biol Med 18(3):145–156

Kelwade JP, Salankar SS (2016) Comparative study of neural networks for prediction of cardiac arrhythmias. In: 2016 International conference on automatic control and dynamic optimization techniques (ICACDOT). https://doi.org/10.1109/icacdot.2016.7877749

Kim J, Wilhelm T (2008) What is a complex graph? Physica A 387(11):2637–2652

Kliouеva IA, van Luijtelaar EL, Chepurnova NE, Chepurnov SA (2001) PTZ-induced seizures in rats: effects of age and strain. Physiol Behav 72(3):421–426

Kristiansen K, Courtois G (1949) Rhythmic electrical activity from isolated cerebral cortex. Electroencephalogr Clin Neurophysiol 1(3):265–272

Kudo M, Sklansky J (2000) Comparison of algorithms that select features for pattern classifiers. Pattern Recognit 33(1):25–41

Lacasa L, Toral R (2010) Description of stochastic and chaotic series using visibility graphs. Phys Rev E 82:036120

Lacasa L, Luque B, Ballesteros F, Luque J, Nuno JC (2008) From time series to complex networks: the visibility graph. Natl Acad Sci USA 105(13):4972–4975

Lacasa L, Luque B, Nuno JC, Luque J (2009) The visibility graph: a new method for estimating the Hurst exponent of fractional Brownian motion. EPL (Europhys Lett) 86(3):30001

Lacasa L, Nunez AM, Roldan E, Parrondo JMR, Luque B (2012) Time series irreversibility: a visibility graph approach. Eur Phys J B 85:1–12. https://doi.org/10.1140/epjb/e2012-20809-8

Last M, Kandel A, Maimon O (2001) Information-theoretic algorithm for feature selection. Pattern Recognit Lett 22(6–7):799–811

Lenjani M, Hashemi MR (2009) A novel arbitration scheme for bandwidth and jitter guarantees in asynchronous NoCs. In: 2009 14th international CSI computer conference. https://doi.org/10.1109/csicc.2009.5349426

Lenjani M, Hashemi MR (2014) Tree-based scheme for reducing shared cache miss rate lever aging regional, statistical and temporal similarities. IET Comput Digital Tech 8(1):30–48

Loscher W, Schmidt D (1988) Which animal models should be used in the search for new antiepileptic drugs? A proposal based on experimental and clinical considerations. Epilepsy Res 2(3):145–181

Luque B, Lacasa L, Balleteros F, Luque J (2009) Horizontal visibility graphs: exact results for random time series. Phys Rev E 80:046103

Luque B, Lacasa L, Ballesteros FJ, Robledo A (2011) Feigenbaum graphs: a complex network perspective of chaos. PLoS One 6:e22411

Makeyev O, Liu X, Luna-Munguía H, Rogel-Salazar G, Mucio-Ramirez S, Liu Y, Sun YL, Kay SM, Besio WG (2012a) Toward a noninvasive automatic seizure control system in rats with transcranial focal stimulations via tripolar concentric ring electrodes. IEEE Trans Neural Syst Rehabil Eng 20(4):422–431

Makeyev O, Liu X, Luna-Munguia H, Rogel-Salazar G, Mucio-Ramirez S, Liu Y, Sun YL, Kay SM, Besio WG (2012) Toward an automatic seizure control system in rats through transcranial focal stimulation via tripolar concentric ring electrodes. In: Proceedings of 65th annual meeting of the American epilepsy society, vol 12, pp 29–30

Mirski MA, Tsai YC, Rossell LA, Thakor NV, Sherman DL (2003) Anterior thalamicmediation of experimental seizures: selective EEG spectral coherence. Epilepsia 44(3):355–365

Mohammadpoory Z, Nasrolahzadeh M, Haddadnia J (2017) Epileptic seizure detection in EEG signals based on the weighted visibility graph entropy. Seizure Eur J Epilepsy 50:202–208

Mohsini KA, Farooq O, Khan YU, Tripathi M (2017) Bispectral analysis of EEG during non-convulsive seizures. In: 2017 international conference on multimedia, signal processing and communication technologies (IMPACT). https://doi.org/10.1109/mspct.2017.8364006

Mookiah MRK, Acharya UR, Lim CM, Petznick A, Suri JS (2012) Data mining technique for automated diagnosis of glaucoma using higher order spectra and wavelet energy features. Knowl-Based Syst 33:73–82

Moxon K, Kuzmick V, Lafferty J, Serfass A, Szperka D, Zale B, Johnson J, Nagvajara P (2001) Real-time seizure detection system using multiple single-neuron recordings. In: 2001 conference proceedings of the 23rd annual international conference of the IEEE engineering in medicine and biology society, Istanbul, Turkey. https://doi.org/10.1109/iembs.2001.1019101

Muni DP, Pal NR, Das J (2006) Genetic programming for simultaneous feature selection and classifier design. IEEE Trans Syst Man Cybern Part B Cybern 36(1):1100–1103

Nakariyakul S, Casasent DP (2009) An improvement on floating search algorithms for feature subset selection. Pattern Recogn 42(9):1932–1940

Nasrolahzadeh M, Mohammadpoori Z, Haddadnia J (2015a) Optimal way to find the frame length of the speech signal for diagnosis of Alzheimer's disease with PSO. Asian J Math Comput Res 2(1):33–41

Nasrolahzadeh M, Mohhamadpoori Z, Haddadnia J (2015b) Adaptive neuro-fuzzy inference system for classification of speech signals in alzheimer's disease using acoustc and non-linear characteristics. Asian J Math Comput Res 3(2):122–131

Nasrolahzadeh M, Mohhamadpoori Z, Haddadnia J (2015c) Alzheimer's disease diagnosis using spontaneous speech signals and hybrid features. Asian J Math Comput Res 7(4):322–331

Nasrolahzadeh M, Mohhamadpoory Z, Haddadnia J (2016) A novel method for early diagnosis of Alzheimer's disease based on higher-order spectral estimation of spontaneous speech signals. Cognit Neurodyn 10(6):495–503

Nasrolahzadeh M, Mohhamadpoory Z, Haddadnia J (2018) Higher-order spectral analysis of spontaneous speech signals in Alzheimer's disease. Cognit Neurodyn 12(6):583–596

Nasrolahzadeh M, Mohammadpoory Z, Haddadnia J (2019) Analysis of heart rate signals during meditation using visibility graph complexity. Cognit Neurodyn 13(1):45–52

Ni XH, Jiang ZQ, Zhou WX (2009) Degree distributions of the visibility graphs mapped from fractional Brownian motions and multifractal random walks. Phys Lett A 373(42):3822–3826

Nicolaou N, Georgiou J (2012) Detection of epileptic electroencephalogram based on permutation entropy and support vector machines. Expert Syst Appl 39(1):202–209

Niknazar M, Mousavi SR, Motaghi S, Dehghani A, Vosoughi Vahdat B, Shamsollahi MB, Sayyah M, Noorbakhsh SM (2013) A unified approach for detection of induced epileptic seizures in rats using ECoG signals. Epilepsy Behav 27(2):355–364

Nunez AM, Lacasa L, Gomez JP, Luque B (2012) Visibility algorithms: a short review. In: Zhang YG (ed.) New frontiers in graph theory. Intech Press, ch. 6

Paul J, Patel CB, Al-Nashash H, Zhang N, Ziai WC, Mirski MA, Sherman DL (2003) Prediction of PTZ-induced seizures using wavelet-based residual entropy of cortical and subcortical field potentials. IEEE Trans Biomed Eng 50(5):640–648

Pei X, Wang J, Deng B, Wei X, Yu H (2014) WLPVG approach to the analysis of EEG-based functional brain network under manual acupuncture. Cognit Neurodyn 8(5):417–428

Polat K, Günes S (2007) Classification of epileptic form EEG using a hybrid system based on decision tree classifier and fast Fourier transform. Appl Math Comput 187(2):1017–1026

Racine RJ (1972) Modification of seizure activity by electrical stimulation: II. Motor seizure. Electroencephalogr Clin Neurophysiol 32(3):281–294

Ramgopal S, Thome-Souza S, Jackson M, Kadish NE, Sánchez Fernández I, Klehm J, Bosl W, Reinsberger C, Schachter S, Loddenkemper T (2014) Seizure detection, seizure prediction, and closed-loop warning systems in epilepsy. Epilepsy Behav 37:291–307

Rubinov M, Sporns O (2010) Complex network measures of brain connectivity: uses and interpretations. NeuroImage 52(3):1059–1069

Schenk J, Kaiser M, Rigoll G (2009) Selecting features in on-line handwritten whiteboard note recognition: SFS or SFFS?. In: 2009 10th international conference on document analysis and recognition. https://doi.org/10.1109/icdar.2009.130

Sherman D, Zhang N, Garg S, Thakor NV, Mirski MA, Anderson Whith M, Hinich MJ (2011) Detection of nonlinear interactions of EEG alpha waves in the brain by a new coherence measure and its application to epilepsy and anti-epileptic drug therapy. Int J Neural Syst 21(2):115–126

Siuly S, Kabir E, Wang H, Zhang Y (2015) Exploring sampling in the detection of multicategory EEG signals. Comput Math Methods Med 2015:1–12

Siuly S, Wang H, Zhang Y (2016) Detection of motor imagery EEG signals employing Naïve Bayes based learning process. Measurement 86:148–158

Srinivas D, Radhakrishnan M, Chakrabarti D, Lakshmegowda M, Manohar N (2018) Intraoperative seizures detected as increased Bispectral Index values during posterior fossa surgeries. J Neuroanaesthesiol Crit Care 5(01):26–29

Srinivasan V, Eswaran C, Siraam N (2007) Approximate entropy based epileptic EEG detection using artificial neural networks. IEEE Trans Inf Technol Biomed 11(3):288–295

Supriya S, Siuly S, Wang H, Cao J, Zhang Y (2016) Weighted visibility graph with complex network features in the detection of epilepsy. IEEE Access 4:6554–6566

Tang X, Xia L, Liao Y, Liu W, Peng Y, Gao T, Zeng Y (2013) New approach to epileptic diagnosis using visibility graph of high-frequency signal. Clin EEG Neurosci 44(2):150–156

Tanq Y, Durand D (2012) A tunable support vector machine assembly classifier for epileptic seizure detection. Exp Syst Appl 39(4):3925–3938

Töllner K, Twele F, Löscher W (2016) Evaluation of the pentylenetetrazole seizure threshold test in epileptic mice as surrogate model for drug testing against pharmacoresistant seizures. Epilepsy Behav 57(Pt A):95–104

Vieira SM, Mendonca LF, Farinha GL, Sousa JMC (2013) Modified binary PSO for feature selection using SVM applied to mortality prediction of septic patients. Appl Soft Comput 13(8):3494–3504

Wang J, Zuo X, He Y (2010) Graph-based network analysis of resting-state functional MRI. Front Syst Neurosci 4:16. https://doi.org/10.3389/fnsys.2010.00016

Xiang J, Li C, Li H, Cao R, Wang B, Han X, Chen J (2015) The detection of epileptic seizure signals based on fuzzy entropy. J Neurosci Methods 243:18–25

Yan J, Wang Y, Ouyang G, Yu T, Li X (2016) Using max entropy ratio of recurrence plot to measure electrocorticogram changes in epilepsy patients. Physica A 443:109–116

Zhou TT, Jin ND, Gao ZK, Luo YB (2012) Limited penetrable visibility graph for establishing complex network from time series. Acta Phys Sin 6(3):030506

Zhu G, Li Y, Wen P (2012) Analysing epileptic EEGs with a visibility graph algorithm. In: 2012 5th international conference on biomedical engineering and informatics. https://doi.org/10.1109/bmei.2012.6513212

Zhu G, Li Y, Wen PP, Wang S (2013) Xi M (2013) Epileptic o genic focus detection in intracranial EEG based on delay permutation entropy. AIP Conf Proc 1559:31. https://doi.org/10.1063/1.4824993

Zhu G, Li Y, Wen PP (2014) Epileptic seizure detection in EEGs signals using a fast weighted horizontal visibility algorithm. Comput Methods Programs Biomed 115(2):64–75